Reflection and transmission of electromagnetic waves on the interface of uniaxial chiral media*

DONG Jian-feng (董建峰), LUO Xiao-yang (罗孝阳), and LI Jie (李杰)**
Institute of Optical Fiber Communication and Network Technology, Ningbo University, Ningbo 315211, China

(Received 4 September 2012)

The reflection and transmission properties of plane waves on the interface of uniaxial chiral media with the optical axis parallel to the interface are investigated. The formulas of the reflected and transmitted power are derived. The curves of the group refractive angles, power of the reflected and transmitted waves for TE and TM incident waves are presented for three cases of dielectric constant combinations and for non-chiral, weak chiral and strong chiral media. Some new results are obtained, which are different from those in the uniaxial chiral media with the optical axis perpendicular to the interface.

Document code: A **Article ID:** 1673-1905(2013)02-0148-5
DOI 10.1007/s11801-013-2349-3

The realization of negative refractive index in the chiral media has attracted much attention in the last decade[1-12]. However, most of the works focus on the isotropic chiral media. In fact, uniaxially anisotropic chiral medium is quite easy to be realized artificially[13]. Recently, negative refractions in uniaxial chiral media (UCM) with the optical axis perpendicular and parallel to the interface have been investigated[14,15]. The reflection and transmission of plane electromagnetic waves in the interface[16] and slab[17] of the UCM with the optical axis perpendicular to the interface have been examined. In this paper, the reflection and transmission properties of plane electromagnetic waves on the interface of UCM with the optical axis parallel to the interface are studied. Some new results different from those in Ref.[16] are obtained.

The constitutive relations in the UCM are[13]

$$\boldsymbol{D}=\boldsymbol{\varepsilon}\cdot\boldsymbol{E}-\mathrm{j}\sqrt{\mu_0\varepsilon_0}\boldsymbol{\kappa}\cdot\boldsymbol{H}, \tag{1}$$

$$\boldsymbol{B}=\boldsymbol{\mu}\cdot\boldsymbol{H}+\mathrm{j}\sqrt{\mu_0\varepsilon_0}\boldsymbol{\kappa}\cdot\boldsymbol{E}, \tag{2}$$

where $\boldsymbol{\varepsilon}=\varepsilon_t\boldsymbol{I}_t+\varepsilon_z\boldsymbol{zz}$, $\boldsymbol{\mu}=\mu_t\boldsymbol{I}_t+\mu_z\boldsymbol{zz}$, $\boldsymbol{I}_t=\boldsymbol{xx}+\boldsymbol{yy}$, $\boldsymbol{\kappa}=\kappa\boldsymbol{zz}$, κ is the chirality parameter, and z is the optical axial direction of the UCM.

A plane electromagnetic wave is obliquely incident at the angle θ_i from free space (ε_0, μ_0) on the interface of the UCM ($\boldsymbol{\varepsilon}$, $\boldsymbol{\mu}$, $\boldsymbol{\kappa}$) with the optical axial parallel to the interface as shown in Fig.1. θ_r is the reflected angle, $\theta_\mathrm{r}=\theta_\mathrm{i}$, and $\theta_\pm$ are the phase refraction angles of two eigenwaves of p^+ wave and p^- wave[13,15] in the UCM. k_i, k_r and $k_\pm$ are the wavenumbers of the incident, reflected and transmitted waves, respectively, and $k_\mathrm{r}=k_\mathrm{i}=k_0=\omega\sqrt{\mu_0\varepsilon_0}$. The wavenumbers of two eigenwaves in the UCM are[13,15]

$$k_\pm=\frac{\omega\sqrt{\varepsilon_t\mu_t}}{\sqrt{\sin^2\theta_\pm+\cos^2\theta_\pm/A_\pm}}, \tag{3}$$

where $A_\pm=\dfrac{1}{2}\left(\dfrac{\mu_z}{\mu_t}+\dfrac{\varepsilon_z}{\varepsilon_t}\right)\pm\sqrt{\dfrac{1}{4}\left(\dfrac{\mu_z}{\mu_t}-\dfrac{\varepsilon_z}{\varepsilon_t}\right)^2+\dfrac{\kappa^2\mu_0\varepsilon_0}{\mu_t\varepsilon_t}}$.

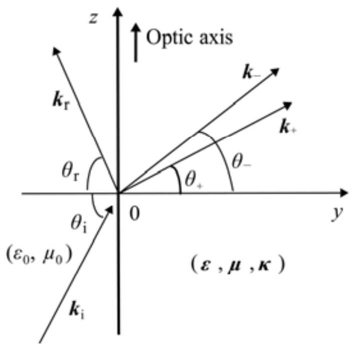

Fig.1 Schematic diagram of the reflection and transmission of a plane wave on the interface of UCM

The electric field of the incident plane wave can be expressed as

$$\boldsymbol{E}_\mathrm{i}=\boldsymbol{E}_{0\mathrm{i}}\exp[-\mathrm{j}k_\mathrm{i}(y\cos\theta_\mathrm{i}+z\sin\theta_\mathrm{i})], \tag{4}$$

where

* This work has been supported by the National Natural Science Foundation of China (No.61078060), the Natural Science Foundation of Zhejiang Province in China (No.Y1091139), the Innovative Research Team Program of Ningbo in China (No.2009B21007), and the K.C. Wong Magna Fund in Ningbo University of China.
** E-mail: dongjianfeng@nbu.edu.cn

$$\boldsymbol{E}_{0\mathrm{i}}=E_{\mathrm{i}\perp}\boldsymbol{x}+E_{\mathrm{i}//}(\boldsymbol{y}\sin\theta_{\mathrm{i}}-\boldsymbol{z}\cos\theta_{\mathrm{i}})\ . \qquad (5)$$

Subscripts ⊥ and // represent perpendicular (TE) and parallel (TM) components of the plane wave, respectively.

The reflected electric fields can be written as

$$\boldsymbol{E}_{\mathrm{r}}=\boldsymbol{E}_{0\mathrm{r}}\exp[-\mathrm{j}k_{\mathrm{r}}(-y\cos\theta_{\mathrm{r}}+z\sin\theta_{\mathrm{r}})]\ , \qquad (6)$$

where

$$\boldsymbol{E}_{0\mathrm{r}}=E_{\mathrm{r}\perp}\boldsymbol{x}+E_{\mathrm{r}//}(\boldsymbol{y}\sin\theta_{\mathrm{r}}+\boldsymbol{z}\cos\theta_{\mathrm{r}})\ . \qquad (7)$$

The electric fields of two transmitted waves can be represented as

$$\boldsymbol{E}_{\pm}=\boldsymbol{E}_{0\pm}\exp[-\mathrm{j}k_{\pm}(y\cos\theta_{\pm}+z\sin\theta_{\pm})]\ , \qquad (8)$$

where[15]

$$\boldsymbol{E}_{0\pm}=E_{0\pm}(\omega\mu_t Y_{z\pm}\boldsymbol{x}+k_{z\pm}\boldsymbol{y}-\frac{k_{y\pm}}{A_{\pm}}\boldsymbol{z})\ , \qquad (9)$$

where $Y_{z\pm}=\dfrac{\varepsilon_t}{-\mathrm{j}\kappa\sqrt{\mu_0\varepsilon_0}}\left(A_{\pm}-\dfrac{\varepsilon_z}{\varepsilon_t}\right)$, $k_{y\pm}=k_{\pm}\cos\theta_{\pm}$ and $k_{z\pm}=k_{\pm}\sin\theta_{\pm}$.

The magnetic fields of the incident, reflected and transmitted waves can be derived from Maxwell's equations. According to the conditions of continuity of the tangent electromagnetic fields on the interface y=0, we obtain $k_{\pm}\sin\theta_{\pm}=k_0\sin\theta_{\mathrm{i}}$. Using Eq.(3), we can find the phase refraction angles $\theta_{\pm}$ and $k_{\pm}$[15]. Then the reflection and transmission matrices of the plane wave on the interface between the UCM and free space can be obtained as

$$\begin{pmatrix}E_{\mathrm{r}\perp}\\E_{\mathrm{r}//}\end{pmatrix}=\begin{bmatrix}R_{11}&R_{12}\\R_{21}&R_{22}\end{bmatrix}\begin{pmatrix}E_{\mathrm{i}\perp}\\E_{\mathrm{i}//}\end{pmatrix}, \qquad (10)$$

$$\begin{pmatrix}E_{0+}\\E_{0-}\end{pmatrix}=\begin{bmatrix}T_{11}&T_{12}\\T_{21}&T_{22}\end{bmatrix}\begin{pmatrix}E_{\mathrm{i}\perp}\\E_{\mathrm{i}//}\end{pmatrix}. \qquad (11)$$

The expressions of the elements in matrices are omitted for simplification.

The time-average Poynting vectors of two transmitted waves can be derived as[15]

$$<\boldsymbol{S}_{\pm}>=\frac{1}{2}\mathrm{Re}\left(\boldsymbol{E}_{\pm}\times\boldsymbol{H}_{\pm}^{*}\right)=\frac{1}{2}\mathrm{Re}[\omega\left|E_{0\pm}\right|^2(\varepsilon_t+\mu_t Y_{z\pm}^2)(\frac{k_{y\pm}}{A_{\pm}}\boldsymbol{y}+k_{z\pm}\boldsymbol{z})]\ . \qquad (12)$$

The relations of the group refraction angles and the phase refraction angles are[15]

$$\theta_{\mathrm{g}\pm}=\tan^{-1}[\frac{\mathrm{Re}(S_z)}{\mathrm{Re}(S_y)}]=\tan^{-1}[A_{\pm}\tan(\theta_{\pm})]\ . \qquad (13)$$

It is noted that the sign of $\theta_{\pm}$ is chosen to ensure that $\mathrm{Re}(S_y)$ is positive.

The normalized reflected power for TE and TM incident waves can be calculated from

$$P_{\mathrm{r}}=|R_{11}|^2+|R_{21}|^2\ (\mathrm{TE}),\quad P_{\mathrm{r}}=|R_{12}|^2+|R_{22}|^2\ (\mathrm{TM})\ . \qquad (14)$$

The normalized power of two transmitted waves for TE and TM incident waves can be calculated from following formulas, respectively

$$P_{t\pm}=\eta_0\omega|(\varepsilon_t+\mu_t Y_{z\pm}^2)|\times\sqrt{|\frac{k_{y\pm}}{A_{\pm}}|^2+|k_{z\pm}|^2}\,|T_{11,21}|^2\frac{\cos(\theta_{\mathrm{g}\pm})}{\cos(\theta_{\mathrm{i}})}\ (\mathrm{TE})\ , \qquad (15)$$

$$P_{t\pm}=\eta_0\omega|(\varepsilon_t+\mu_t Y_{z\pm}^2)|\sqrt{|\frac{k_{y\pm}}{A_{\pm}}|^2+|k_{z\pm}|^2}\times|T_{12,22}|^2\frac{\cos(\theta_{\mathrm{g}\pm})}{\cos(\theta_{\mathrm{i}})}\ (\mathrm{TM})\ . \qquad (16)$$

In the following calculation, we assume $\mu_t=\mu_z=\mu_0$ and $\omega/2\pi$=5 GHz. We analyze and discuss the reflection and transmission properties of plane waves on the interface of UCM with the optical axis parallel to the interface for three cases of dielectric constant combinations and for non-chiral (κ=10^{-6} in calculation), weak chiral (small chirality parameter $\kappa<\sqrt{\mu_z\varepsilon_z/\mu_0\varepsilon_0}$) and strong chiral (large chirality parameter $\kappa>\sqrt{\mu_z\varepsilon_z/\mu_0\varepsilon_0}$) media.

For the case of $\varepsilon_t>0,\ \varepsilon_z>0$, because the refractive angles of the plane wave in the UCM are quite different for $\mu_t\varepsilon_t<\mu_0\varepsilon_0$ and $\mu_t\varepsilon_t>\mu_0\varepsilon_0$ [15], we discuss these two cases, respectively.

Fig.2(a) presents the group refractive angles $\theta_{\mathrm{g}\pm}$ versus the incidence angle θ_{i} for different chiral parameters in the case of $\varepsilon_t>0$, $\varepsilon_z>0$ and $\mu_t\varepsilon_t<\mu_0\varepsilon_0$ ($\varepsilon_t=0.6\varepsilon_0$, $\varepsilon_z=2\varepsilon_0$). For non-chiral ($\kappa$=$10^{-6}$ in calculation) and small chirality parameter (κ=0.5, $\kappa<\sqrt{\mu_z\varepsilon_z/\mu_0\varepsilon_0}$), $\theta_{\mathrm{g}\pm}$ increases as θ_{i} increases, and $\theta_{\mathrm{g}+}>\theta_{\mathrm{g}-}$. When $\theta_{\mathrm{i}}=50.8°$ (the critical angle $\sin^{-1}\sqrt{\mu_t\varepsilon_t/\mu_0\varepsilon_0}$), $\theta_{\mathrm{g}\pm}=90°$, and total internal reflection (TIR) occurs for p^+ and p^- waves. For large chirality parameter (κ=1.5, $\kappa>\sqrt{\mu_z\varepsilon_z/\mu_0\varepsilon_0}$), when $\theta_{\mathrm{i}}<50.8°$, only p^+ wave can propagate, $\theta_{\mathrm{g}+}$ increases as θ_{i} increases, and when $\theta_{\mathrm{i}}>50.8°$, only p^- wave can propagate, $\theta_{\mathrm{g}-}$ decreases as θ_{i} increases.

Fig.2(b) shows the normalized reflected power P_{r} versus θ_{i}. For κ=0.5, P_{r} is almost the same as that in non-chiral case. As θ_{i} approaches the critical angle, P_{r} increases rapidly, and when θ_{i} is equal to or greater than the critical angle, P_{r} =1, i.e., TIR occurs. For κ=1.5, when θ_{i} equals the critical angle, TIR occurs for TE and TM waves. When θ_{i} is greater than the critical angle, P_{r} decreases rapidly first and then increases monotonously.

The normalized transmitted power $P_{t\pm}$ for TE and TM incident waves are shown in Fig.2(c) and (d). It is found that $P_{\mathrm{r}}+P_{t+}+P_{t-}=1$. For κ=10^{-6} and 0.5, the transmitted wave is mostly p^- wave for TE incident wave and p^+

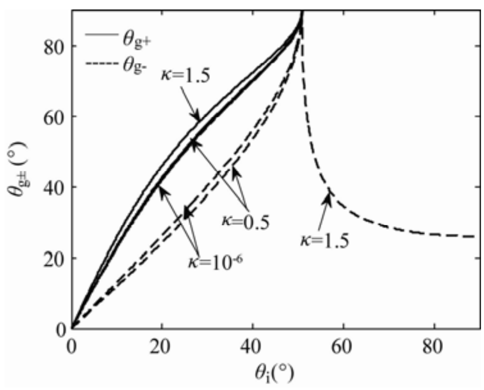

(a) Group refractive angles

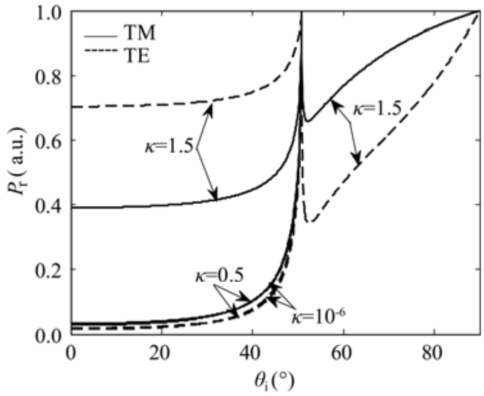

(b) Normalized reflected power

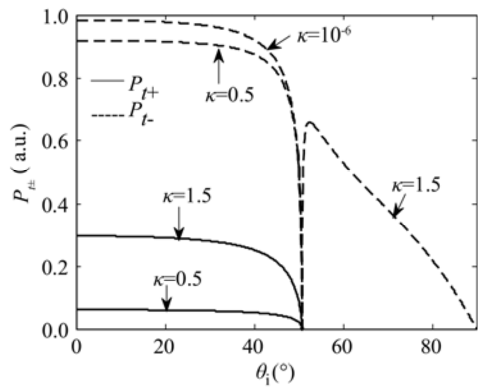

(c) Normalized transmitted power for TE incident wave

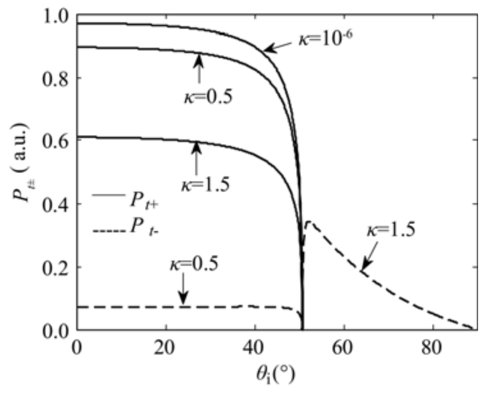

(d) Normalized transmitted power for TM incident wave

Fig.2 Parameters in the case of ε_t>0, ε_z>0 and $\mu_t\varepsilon_t$< $\mu_0\varepsilon_0$ (ε_t= 0.6ε_0, ε_z=2ε_0)

wave for TM incident wave. For κ=1.5, when $\theta_i < 50.8°$, P_{t+} for TE incident wave is less than that for TM incident wave, and when $\theta_i > 50.8°$, P_{t-} for TE incident wave is greater than that for TM incident wave.

In the case of $\varepsilon_t > 0$, $\varepsilon_z > 0$ and $\mu_t\varepsilon_t > \mu_0\varepsilon_0$, for nonchiral and small chirality parameter media, both p^+ and p^- waves always exist for any θ_i, and there exists Brewster's angle (P_r=0) for TM incident wave. For large κ, only p^+ wave can propagate, and there is no Brewster's angle for TE and TM incident waves.

Fig.3(a) presents $\theta_{g\pm}$ versus θ_i for $\varepsilon_t < 0$, $\varepsilon_z > 0$ ($\varepsilon_t = -0.5\varepsilon_0$, $\varepsilon_z = 2\varepsilon_0$). It can be shown that when κ becomes zero, p^+ and p^- waves correspond to TE and TM waves, respectively. For κ=10^{-6} and 0.5, only p^- wave exists. θ_{g-} is negative, and $|\theta_{g-}|$ increases as θ_i increases. For κ=1.5, both p^+ and p^- waves exist, θ_{g+} is positive and increases as θ_i increases, and $\theta_{g+} < |\theta_{g-}|$, so the two transmitted waves are totally split. Fig.3(b) shows P_r versus θ_i. For κ=10^{-6}, at any θ_i, TIR always occurs for TE incident wave, because only TM wave can propagate in the UCM. Brewster's angle exists for TM incident wave. For κ=0.5, P_r is still large for TE incident wave. However, P_r appears as the minimum (not equal to zero) for TM incident wave. For κ=1.5, the difference of P_r is very small for TE and TM incident waves.

$P_{t\pm}$ for TE and TM incident waves are shown in Fig.3 (c) and (d). For κ=10^{-6}, there is no transmitted wave for TE incident wave. For κ=0.5, P_{t-} is small for TE incident wave and large for TM incident wave. For κ=1.5, $P_{t+} > P_{t-}$ for TE incident wave, and the difference decreases as θ_i increases, but $P_{t+} = P_{t-}$ for TM incident wave. In the range of θ_i =37°−65°, $P_{t+} \approx 0$. From above discussion on the sign of the group refractive angles and values of the transmitted power, it can be seen that the UCM with large chirality parameter is suitable to split TE incident wave.

Fig.4(a) shows $\theta_{g\pm}$ versus θ_i for $\varepsilon_t > 0$, $\varepsilon_z < 0$ and $\mu_t\varepsilon_t < \mu_0\varepsilon_0$ ($\varepsilon_t = 0.4\varepsilon_0$, $\varepsilon_z = -2\varepsilon_0$). It can also be shown that when κ becomes zero, p^+ and p^- waves correspond to TE and TM waves, respectively. When θ_i<39.2°, only p^+ wave can propagate, and θ_{g+} increases as θ_i increases. When θ_i>39.2°, only p^- wave can propagate, and θ_{g-} decreases as θ_i increases. Fig.4(b) presents P_r versus θ_i. For κ=10^{-6}, TIR occurs when θ_i>39.2° for TE incident wave, and when θ_i<39.2° for TM incident wave. There exists Brewster's angle when $\theta_i > 39.2°$ for TM incident wave. For κ=0.5, TIR and Brewster's angle disappear. Fig.4(c) and (d) show $P_{t\pm}$ for TE and TM incident waves, respectively. For κ=10^{-6}, total transmission occurs for TM incident wave.

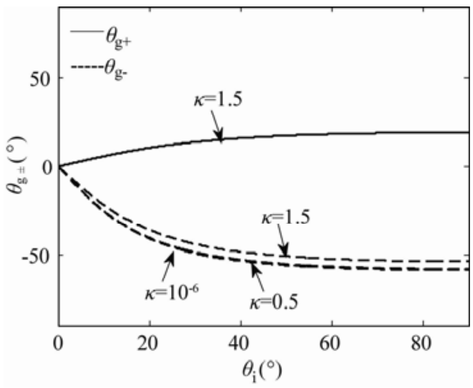

(a) Group refractive angles

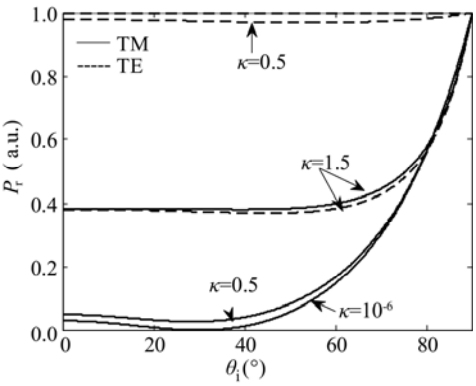

(b) Normalized reflected power

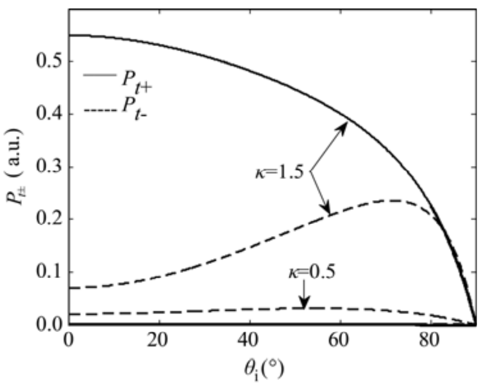

(c) Normalized transmitted power for TE incident wave

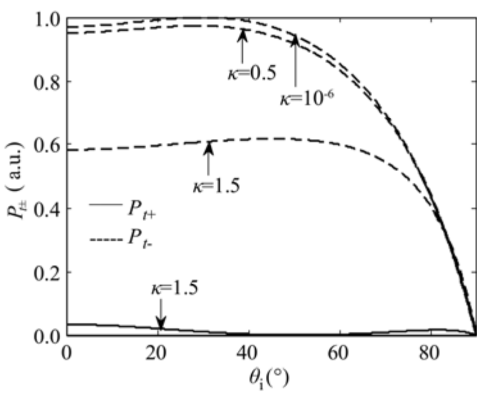

(d) Normalized transmitted power for TM incident power

Fig.3 Parameters in the case of ε_t<0, ε_z>0 (ε_t= -0.5ε_0, ε_z=2ε_0)

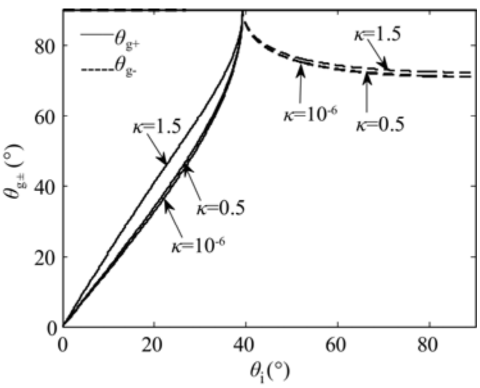

(a) Group refractive angles

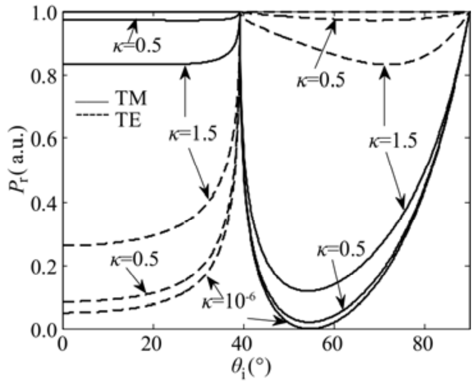

(b) Normalized reflected power

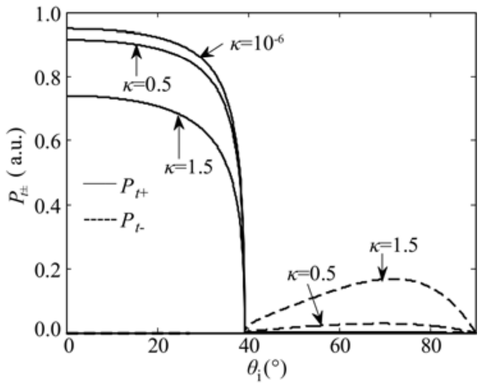

(c) Normalized transmitted power for TE incident wave

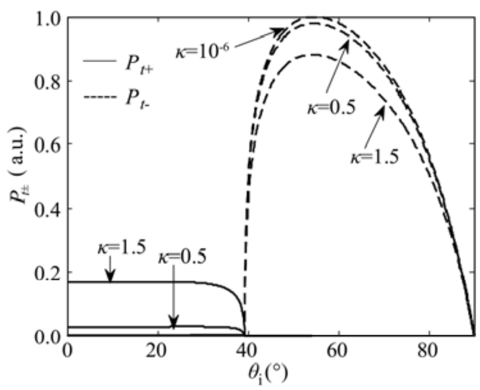

(d) Normalized transmitted power for TM incident wave

Fig.4 Parameters in the case of ε_t>0, ε_z<0 and $\mu_t\varepsilon_t$< $\mu_0\varepsilon_0$ (ε_t= 0.4ε_0, ε_z=-2ε_0)

For $\varepsilon_t > 0$, $\varepsilon_z < 0$ and $\mu_t\varepsilon_t > \mu_0\varepsilon_0$, only p^+ wave can exist. For non-chiral media, TIR always occurs for TM incident wave.

In summary, the reflection and transmission properties of plane electromagnetic waves on the interface of the UCM with the optical axis parallel to the interface are investigated. The formulas of the power of reflected wave and two transmitted eigenwaves are derived. The curves of the group refractive angles, power of the reflected and transmitted waves for TE and TM incident waves are given for three cases of dielectric constant combinations and for non-chiral, weak chiral and strong chiral media. The results show that for $\varepsilon_t > 0$, $\varepsilon_z > 0$ case, only when $\mu_t\varepsilon_t > \mu_0\varepsilon_0$, there exists Brewster's angle for non-chiral and small chirality parameter media for TM incident wave. For $\varepsilon_t < 0$, $\varepsilon_z > 0$ case and $\varepsilon_t > 0$, $\varepsilon_z < 0$ case, Brewster's angle emerges only for non-chiral media and for TM incident wave. Especially, for $\varepsilon_t < 0$, $\varepsilon_z > 0$ case, the UCM with large chirality parameter can split TE incident wave. These results are quite different from those in the UCM with the optical axis perpendicular to the interface[16].

References

[1] Pendry J. B., Science **306**, 1353 (2004).

[2] Tretyakov S., Sihvola A. and Jylhä L., Photonics Nanostruct. **3**, 107 (2005).

[3] Monzon C. and Forester D. W., Phys. Rev. Lett. **95**, 123904 (2005).

[4] Jin Y. and He S. L., Opt. Express **13**, 4974 (2005).

[5] Plum E., Zhou J., Dong J., Fedotov V. A., Koschny T., Soukoulis C. M. and Zheludev N. I., Phys. Rev. B **79**, 035407 (2009).

[6] S. Zhang, Y. Park, J. Li, X. Lu, W. Zhang and X. Zhang, Phys. Rev. Lett. **102**, 023901 (2009).

[7] Zhou J., Dong J., Wang B., Koschny T., Kafesaki M. and Soukoulis C. M., Phys. Rev. B **79**, 121104 (2009).

[8] Wiltshire M. C. K., Pendry J. B. and Hajnal J. V., J. Phys.: Condens. Matter **21**, 292201 (2009).

[9] Dong J., Zhou J., Koschny T. and Soukoulis C., Opt. Express **17**, 14172 (2009).

[10] Li J., Yang F. Q. and Dong J. F., Prog. Electromagn. Res. **116**, 395 (2011).

[11] XU Chao and DONG Jian-feng, J. Optoelectron. Laser **21**, 1528 (2010). (in Chinese)

[12] DONG Jian-feng and YANG Fang-qing, J. Optoelectron. Laser **22**, 237 (2011). (in Chinese)

[13] Lindell I. V., Sihvola A. H., Tretyakov S. A. and Viitanen A. J., Electromagnetic Waves in Chiral and Bi-isotropic Media, Boston: Artech House Publishers, 275 (1994).

[14] Cheng Q. and Cui T. J., Phys. Rev. B **73**, 113104 (2006).

[15] LI Jie and DONG Jian-Feng, Acta Phys. Sin. **61**, 114101 (2012). (in Chinese)

[16] Cheng Q. and Cui T. J., J. Opt. Soc. Am. A **23**, 3203 (2006).

[17] Dong J. F. and Li J., Prog. Electromagn. Res. **127**, 389 (2012).